DALTON
FULL PAPER

Syntheses, crystal structures and magnetic properties of di- and trinuclear croconato-bridged copper(II) complexes

Isabel Castro,[a] María Luisa Calatayud,[a] Francesc Lloret,[a] Jorunn Sletten[b] and Miguel Julve*[a]

[a] *Departament de Química Inorgànica/Instituto de Ciencia Molecular, Universitat de València, Dr. Moliner 50, 46100 Burjassot, València, Spain. E-mail: miguel.julve@uv.es*
[b] *Department of Chemistry, University of Bergen, N-5007 Bergen, Norway. E-mail: jorunn.sletten@kj.uib.no*

Received 29th January 2002, Accepted 28th March 2002
First published as an Advance Article on the web 2nd May 2002

The new croconato-bridged copper(II) compounds $[Cu_2(terpy)_2(H_2O)_2(C_5O_5)](NO_3)_2{\cdot}H_2O$ (**1**) and $[Cu_3(phen)_5(C_5O_5)_2](CF_3SO_3)_2$ (**2**) ($C_5O_5^{2-}$ = croconate, dianion of 4,5-dihydroxycyclopent-4-ene-1,2,3-trione; terpy = 2,2′:6′,2″-terpyridine; phen = 1,10-phenanthroline) have been prepared, and their crystal structures and variable temperature magnetic susceptibilities determined. The structure of complex **1** consists of croconato-bridged dinuclear $[Cu_2(terpy)_2(H_2O)_2(C_5O_5)]^{2+}$ complex ions, nitrate counter ions and water of hydration. The croconato ligand exhibits an asymmetrical bis-bidentate coordination mode through four of its five oxygen atoms. The two crystallographically independent copper atoms have similar coordination geometries: elongated, distorted octahedral with three terpyridyl nitrogen atoms and one croconate oxygen atom in the equatorial plane, and a second croconate oxygen atom and a water molecule in the axial positions, the stronger axial interaction in each case being to the water molecule. The intramolecular copper–copper separation across the croconate bridge is 6.852(1) Å. The structure of complex **2** is built of croconato-bridged trinuclear $[Cu_3(phen)_5(C_5O_5)_2]^{2+}$ complex ions and triflate counter ions. The terminal copper atoms [Cu(1) and Cu(1a)] have, to the first approximation, a square pyramidal coordination geometry with one croconate oxygen and three phen nitrogen atoms in equatorial positions, and a fourth phen nitrogen atom in the apical position. A second semi-coordinated croconate oxygen atom is located in the remaining axial position. The central copper atom [Cu(2)] is elongated octahedral with two croconate oxygen and two phen nitrogen atoms in equatorial positions, and two oxygen atoms, one from each croconate group, in axial positions. The croconate ligands in **2** adopt an unusual asymmetrical bis-bidentate bridging mode involving three adjacent oxygen atoms, the copper–copper separation across this bridge being 4.177(1) Å. Variable temperature magnetic susceptibility measurements show the occurrence of weak [$J = -2.94$ cm^{-1} (**1**)] and intermediate [$J = -47.1$ cm^{-1} (**2**)] intramolecular antiferromagnetic interactions across the bridging croconato. These values are analyzed in the light of their structures and compared with those previously reported for the parent compounds.

Introduction

Although diprotic croconic acid ($H_2C_5O_5$, 4,5-dihydroxycyclopent-4-ene-1,2,3-trione) and its potassium salt were first isolated in 1825 by Gmelin,[1] the crystal structure of the potassium croconate dihydrate was only published 175 years later.[2] The predictions made on the formation of sandwich complexes with ring-bonding from croconate to transition metal ions, based on the close to D_{5h} symmetry which the croconate exhibits in its potassium,[2] lithium[3] and ammonium[4] salts, were not realised.[5–7] In fact, recent theoretical calculations have revealed the very low aromatic character of the croconate dianion.[8] Studies of complex formation between croconate and the preformed copper(II) complexes $[CuL]^{(2-l)+}$ (L = bi- and tridentate nitrogen donors) in dimethyl sulfoxide solution,[9] which were also extended to the related oxalate ($C_2O_4^{2-}$)[10–12] and squarate ($C_4O_4^{2-}$)[13] ligands, identified a closer similarity between croconate and oxalate than between the two cyclic oxocarbon dianions. So, whereas the squarato complexes are much less stable and their stability constants suggest monodentate coordination of this ligand, those of the croconato and oxalato complexes are several orders of magnitude higher, supporting a chelating coordination mode for them. X-Ray studies on single crystals of these complexes[9–17] confirmed the conclusions obtained from the solution studies; the high bite parameter for the squarate causes this difference in the coordinating behaviour of squarate *versus* that of croconate and oxalate.[14]

The structural data of the croconate complexes with transition metal ions show that this ligand can coordinate to the metal ions as a terminal bidentate (**I**, Scheme 1),[9,16,18–23] bridging bidentate/monodentate (**II**, Scheme 1)[6,7,24] or bridging bis-bidentate ligand through either four (**III**, Scheme 1)[15,25] or three adjacent (**IV**, Scheme 1)[26,27] croconate oxygen atoms.

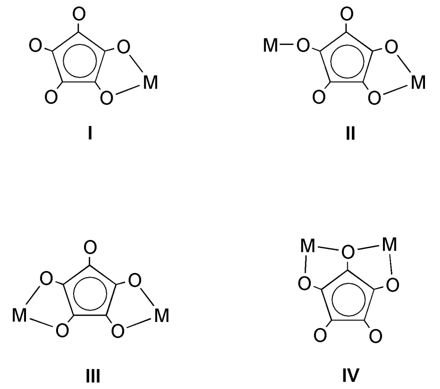

Scheme 1

Monodenate and bis-monodentate coordination modes of croconate were observed, in addition to **I**, **III** and **IV**, in its complexes with rare-earth cations.[28–31]

DOI: 10.1039/b201090a

In the present work, we focus on two croconato-bridged copper(II) compounds of formulae $[Cu_2(terpy)_2(H_2O)_2(C_5O_5)](NO_3)_2\cdot H_2O$ (**1**) (dinuclear) and $[Cu_3(phen)_5(C_5O_5)_2](CF_3SO_3)_2$ (**2**) (trinuclear) (terpy = 2,2′:6′,2″-terpyridine and phen = 1,10-phenanthroline) which were grown from aqueous solutions containing croconate and the preformed $[Cu(terpy)]^{2+}$ and $[Cu(phen)_2]^{2+}$ species. The rare bridging modes **III** (**1**) and **IV** (**2**) are observed in these compounds. The syntheses, crystal structure determinations and magnetic susceptibility studies of **1** and **2** have been performed.

Experimental

Materials

1,10-Phenanthroline monohydrate, 2,2′:6′,2″-terpyridine, copper(II) nitrate trihydrate and copper(II) triflate were purchased from commercial sources and used as received. Anhydrous potassium croconate was prepared by reported procedures.[32] Elemental analyses (C, H, N) were conducted by the Microanalytical Service of the Universidad Autónoma de Madrid.

Preparations

$[Cu_2(terpy)_2(H_2O)_2(C_5O_5)](NO_3)_2\cdot H_2O$ (1). 1 mmol of terpy (0.233 g), 1 mmol of $Cu(NO_3)_2\cdot 3H_2O$ (0.296 g) and 3 mmol of $NaNO_3$ (0.255 g) were dissolved in 75 cm^3 of hot water with stirring. The addition of 0.5 mmol of potassium croconate (0.109 g, 0.5 mmol) dissolved in the minimum amount of water was accompanied by a colour change of the solution from blue to green. Green polyhedral crystals of **1** suitable for X-ray diffraction analysis were obtained from this solution by slow evaporation at room temperature. The yield was 90% (Found: C, 45.93; H, 3.01; N, 12.15; calc. for $C_{35}H_{28}Cu_2N_8O_{14}$: C, 46.12; H, 3.07; N, 12.29%).

$[Cu_3(phen)_5(C_5O_5)_2](CF_3SO_3)_2$ (2). 1.66 mmol of phen (0.300 g) dissolved in 150 cm^3 of ethanol were added to a warm aqueous solution of 1 mmol of copper(II) triflate (0.213 g, 50 cm^3). The addition of 0.66 mmol of potassium croconate (0.145 g) was accompanied by a colour change of the solution from blue to green and by subsequent formation of a green powder. Green polyhedral crystals of **2** suitable for X-ray analysis were obtained as the main product from the remaining solution by slow evaporation at room temperature. A small amount of blue crystals of the tris-chelated $[Cu(phen)_3](CF_3SO_3)_2\cdot H_2O$[33] compound were also obtained. The yield was 60% (Found: C, 51.45; H, 2.36; N, 8.31; calc. for $C_{72}H_{40}Cu_3F_6N_{10}O_{16}S_2$: C, 51.76; H, 2.40; N, 8.38%).

Physical techniques

Infrared spectra were recorded on a Perkin–Elmer 1750 FTIR spectrophotometer from KBr pellets in the 4000–400 cm^{-1} region. The magnetic susceptibilities of polycrystalline samples were measured over the temperature range 1.8–290 K with a Quantum Design SQUID susceptometer using an applied magnetic field of 0.1 T. Mercury tetrakis(thiocyanato)-cobaltate(II) was used as a susceptibility standard. Diamagnetic corrections of the constituent atoms were estimated from Pascal's constants and found to be -413×10^{-6} (**1**) and -851×10^{-6} cm^3 mol^{-1} (**2**) per two (**1**) and three (**2**) copper(II) ions, respectively.[34] A value of 60×10^{-6} cm^3 mol^{-1} was used for the temperature independent paramagnetism of the copper(II) ion.

Crystallography

Diffraction data for compound **1** were collected at 293 K using an Enraf-Nonius CAD-4 diffractometer and for compound **2** at 173 K using a SMART 2K CCD area detector diffractometer, equipped with an Oxford Cryostream N_2 cooling device.[35] Crystal parameters and refinement results are summarized in Table 1. In the case of **1**, a decay amounting to in average 4% was observed during data collection and was corrected for. Empirical absorption corrections were carried out based on ψ-scan measurements of 7 reflections for **1**,[36] and by SADABS for **2**.[37] The structures were solved by direct methods and refined by full matrix least squares based on F^2, including all reflections. In the case of compound **1**, all non-hydrogen atoms were refined anisotropically, whereas, for compound **2**, carbon atoms were refined isotropically. The latter choice was made because one of the carbon atoms obtained a none positive definite temperature factor, and that the introduction of a large number of extra refinement prameters led to an increase in standard deviations in bond lengths and angles. Hydrogen atoms bound to carbon were included in the model at idealized positions, while, in the case of **1**, hydrogen atoms bound to coordinated oxygen (water) were located in Fourier difference maps and were refined according to the riding model. Hydrogen atoms of the non-coordinated water molecule could not be located.

Data collection and data reduction for **1** were carried out with the CAD4-Express and XCAD programs,[38] whereas, for **2**, the SMART and SAINT programs[39] were used. All other calculations were performed with the SHELXS 86, SHELXL/PC and XP programs.[40] Selected bond distances and angles are listed in Tables 2–3.

CCDC reference numbers 178404 and 178405.

See http://www.rsc.org/suppdata/dt/b2/b201090a/ for crystallographic data in CIF or other electronic format.

Results and discussion

Structures

$[Cu_2(terpy)_2(H_2O)_2(C_5O_5)](NO_3)_2\cdot H_2O$ (1). The structure of **1** consists of croconato-bridged dinuclear $[Cu_2(terpy)_2(H_2O)_2(C_5O_5)]^{2+}$ cations (Fig. 1), nitrate counter ions and water of hydration. Cations separated by a unit cell translation along the *a*-axis are connected through a hydrogen bond between the coordinated water molecule O(6) and the croconate oxygen O(4) [2.932(4) Å for O(6) ··· O(4a); (a) $x - 1, y, z$]. The nitrate ions form hydrogen bonds to the coordinated water molecules, the O ··· O distances varying in the range 2.720(8)–3.077(7) Å (see end of Table 2).

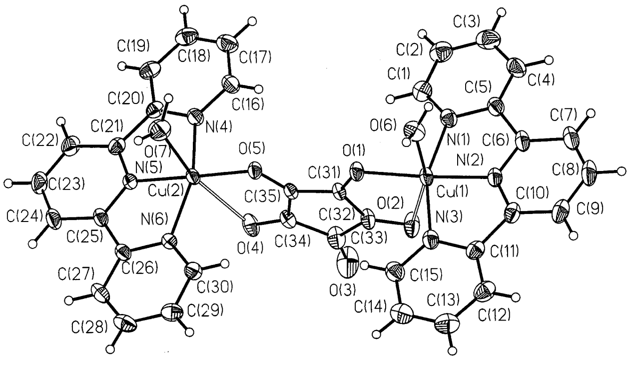

Fig. 1 The dinuclear complex unit $[Cu_2(terpy)_2(H_2O)_2(C_5O_5)]^{2+}$ in **1**. Thermal ellipsoids are plotted at the 30% probability level.

The two crystallographically independent copper atoms have similar coordination geometries: elongated, distorted octahedral with terpyridyl nitrogen atoms and one croconate oxygen atom in the equatorial plane {Cu–N bond distances in the ranges 1.937(3)–2.047(4) [Cu(1)] and 1.944(3)–2.038(3) Å [Cu(2)] and Cu–O bond lengths of 1.959(3) [Cu(1)] and 1.955(3) Å [Cu(2)]}, and a second croconate oxygen atom {Cu–O = 2.529(3) [Cu(1)] and 2.597(3) Å [Cu(2)]} and a water molecule {Cu–O = 2.425(3) [Cu(1)] and 2.350(3) Å [Cu(2)]} in

Table 1 Summary of crystallographic data and structure refinement for $[Cu_2(terpy)_2(H_2O)_2(C_5O_5)](NO_3)_2\cdot H_2O$ (**1**) and $[Cu_3(phen)_5(C_5O_5)_2](CF_3SO_3)_2$ (**2**)

	1	**2**
Formula	$C_{35}H_{28}Cu_2N_8O_{14}$	$C_{72}H_{40}Cu_3F_6N_{10}O_{16}S_2$
M	911.73	1669.88
Temperature/K	293(2)	173
λ/Å	0.71073	0.71073
Crystal system	Triclinic	Monoclinic
Space group	$P\bar{1}$	$C2/c$
a/Å	9.5413(14)	28.2425(6)
b/Å	13.473(2)	10.9029(5)
c/Å	15.059(2)	21.8194(9)
α/°	86.678(12)	90
β/°	72.591(12)	102.604(2)
γ/°	79.610(12)	90
V/Å^3	1816.9(5)	6556.8(4)
Z	2	4
ρ/g cm^{-3}	1.667	1.692
μ/mm^{-1}	1.254	1.127
Max 2θ/°	47.9	50
Reflections collected	6037	19107
Independent reflections (R_{int})	5648 (0.0172)	5762 (0.1339)
Reflections with $I > 2\sigma(I)$	4484	2392
Data/restraints/parameters	5648/0/532	5691/0/312
R [$I > 2\sigma(I)$]	0.0444	0.0873
R_w [$I > 2\sigma(I)$]	0.1102	0.1464
S	1.018	0.997

Table 2 Selected bond lengths (Å) and angles (°) for $[Cu_2(terpy)_2(H_2O)_2(C_5O_5)](NO_3)_2\cdot H_2O$ (**1**), with e.s.d.s in parentheses

Copper coordination spheres

Cu(1)–N(2)	1.937(3)	Cu(2)–N(5)	1.944(3)
Cu(1)–O(1)	1.959(3)	Cu(2)–O(5)	1.955(3)
Cu(1)–N(3)	2.024(4)	Cu(2)–N(4)	2.036(3)
Cu(1)–N(1)	2.047(4)	Cu(2)–N(6)	2.038(3)
Cu(1)–O(6)	2.425(3)	Cu(2)–O(7)	2.350(3)
Cu(1)–O(2)	2.529(3)	Cu(2)–O(4)	2.597(3)
N(2)–Cu(1)–O(1)	174.66(13)	N(5)–Cu(2)–O(5)	178.56(13)
N(2)–Cu(1)–N(3)	80.04(15)	N(5)–Cu(2)–N(4)	79.79(14)
O(1)–Cu(1)–N(3)	100.80(13)	O(5)–Cu(2)–N(4)	99.92(13)
N(2)–Cu(1)–N(1)	79.68(15)	N(5)–Cu(2)–N(6)	79.64(13)
O(1)–Cu(1)–N(1)	99.94(13)	O(5)–Cu(2)–N(6)	100.74(12)
N(3)–Cu(1)–N(1)	158.89(14)	N(4)–Cu(2)–N(6)	159.05(13)
N(2)–Cu(1)–O(6)	88.56(13)	N(5)–Cu(2)–O(7)	90.18(13)
O(1)–Cu(1)–O(6)	86.16(11)	O(5)–Cu(2)–O(7)	88.42(12)
N(3)–Cu(1)–O(6)	90.21(13)	N(4)–Cu(2)–O(7)	91.36(13)
N(1)–Cu(1)–O(6)	95.07(12)	N(6)–Cu(2)–O(7)	92.63(13)
N(2)–Cu(1)–O(2)	108.49(12)	N(5)–Cu(2)–O(4)	105.55(12)
O(1)–Cu(1)–O(2)	76.82(11)	O(5)–Cu(2)–O(4)	75.85(10)
N(3)–Cu(1)–O(2)	90.57(13)	N(4)–Cu(2)–O(4)	91.67(12)
N(1)–Cu(1)–O(2)	90.34(13)	N(6)–Cu(2)–O(4)	90.04(12)
O(6)–Cu(1)–O(2)	162.80(11)	O(7)–Cu(2)–O(4)	164.27(11)

Hydrogen bonds[a,b]

D	H	A	D ··· A/Å	H ··· A/Å	D–H ··· A/°
O(6)	H(62)	O(4a)	2.932(4)	1.99	172
O(6)	H(61)	O(10a)	2.888(8)	2.12	155
O(7)	H(71)	O(8b)	2.720(8)	1.77	172
O(7)	H(72)	O(12c)	2.973(7)	2.18	149
O(7)	H(72)	O(13c)	3.077(7)	2.29	149

[a] D = donor and A = acceptor. [b] Symmetry operations used to generate equivalent atoms: (a) $x - 1, y, z$; (b) $1 - x, 1 - y, 1 - z$; (c) $1 - x, 1 - y, 1 - z$.

Table 3 Selected bond lengths (Å) and angles (°) for $[Cu_3(phen)_5(C_5O_5)_2](CF_3SO_3)_2$ (**2**), with e.s.d.s in parentheses

Copper coordination spheres[a]

Cu(1)–O(1)	1.970(5)	Cu(1)–O(5)	2.875(7)
Cu(1)–N(4)	2.009(7)	Cu(2)–O(2)	1.974(6)
Cu(1)–N(2)	2.015(7)	Cu(2)–N(5)	2.002(7)
Cu(1)–N(1)	2.016(7)	Cu(2)–O(1)	2.484(5)
Cu(1)–N(3)	2.241(7)		
O(1)–Cu(1)–N(4)	92.3(3)	N(1)–Cu(1)–O(5)	91.4(2)
O(1)–Cu(1)–N(2)	167.5(3)	N(3)–Cu(1)–O(5)	162.5(2)
N(4)–Cu(1)–N(2)	93.1(3)	O(2a)–Cu(2)–O(2)	92.1(3)
O(1)–Cu(1)–N(1)	92.8(3)	O(2a)–Cu(2)–N(5a)	94.8(3)
N(4)–Cu(1)–N(1)	174.8(3)	O(2)–Cu(2)–N(5a)	163.9(3)
N(2)–Cu(1)–N(1)	82.0(3)	O(2)–Cu(2)–N(5)	94.8(3)
O(1)–Cu(1)–N(3)	93.8(2)	N(5a)–Cu(2)–N(5)	82.4(4)
N(4)–Cu(1)–N(3)	79.4(3)	O(2a)–Cu(2)–O(1)	82.1(2)
N(2)–Cu(1)–N(3)	98.3(3)	O(2)–Cu(2)–O(1)	77.6(2)
N(1)–Cu(1)–N(3)	99.4(3)	N(5a)–Cu(2)–O(1)	117.8(2)
O(1)–Cu(1)–O(5)	71.9(2)	N(5)–Cu(2)–O(1)	85.2(2)
N(4)–Cu(1)–O(5)	91.0(2)	O(1)–Cu(2)–O(1a)	150.6(3)
N(2)–Cu(1)–O(5)	96.8(2)		

[a] Symmetry transformations used to generate equivalent atoms: (a) $-x, y, -z + 0.5$.

the axial positions, the stronger axial interaction in each case being to the water molecule. The Cu–N bond of the central pyridyl ring of the terpy ligand is significantly shorter than those of the outer pyridyl rings, as previously observed in other terpyridyl-containing copper(II) complexes.[12,14,41–44] The values of the angles subtended by the tridentate terpy at each copper atom [79.68(15) and 80.04(15)° at Cu(1) and 79.79(14) and 79.64(13)° at Cu(2)] deviate significantly from the ideal value of 90° due to the small bite size of the five-membered planar chelate rings. The dihedral angle between the planes defined by the equatorial ligand atoms of Cu(1) and Cu(2) is 18.8°, the copper atoms deviating by only 0.004 [Cu(1)] and 0.020 Å [Cu(2)] from their equatorial planes [in the direction of the axial water ligand in the case of Cu(2)].

The individual pyridine rings of the terpy ligand are planar [maximum deviation 0.012 Å at C(3) and C(28)]. However, the ligand as a whole is not planar, showing dihedral angles of 4.1 and 3.3° [terpy bound at Cu(1)], and 5.1 and 0.3° [terpy bound at Cu(2)] between its two outer rings and the central ring. Average C–C bond distances within the rings [1.379(8) Å], C–N bonds [1.345(8) Å] and inter-ring C–C bonds [1.480(3) Å] compare well with previously reported data.[12,14,41–44] Two of the pyridine rings of each terpy ligand partially overlap with corresponding rings in centrosymetrically related neighbour molecules, giving a certain degree of π–π interaction (see Fig. 2) [average distance between overlapping rings at the Cu(1) side

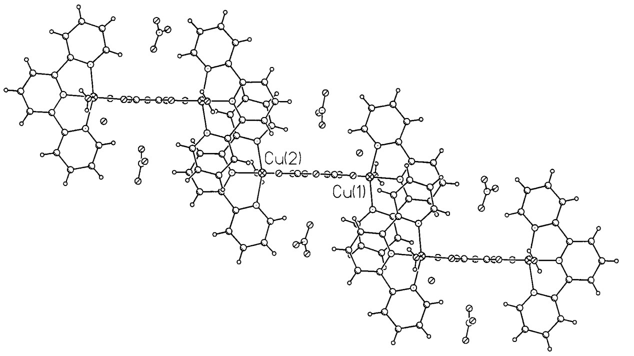

Fig. 2 A view of the π–π interactions between neighbouring terpy ligands in **1**.

being 3.54 Å (rings at *x*, *y*, *z* and $-x$, $1 - y$, $2 - z$) and at the Cu(2) side being 3.46 Å (rings at *x*, *y*, *z* and $2 - x$, $-y$, $1 - z$)]. The bridging croconate group is essentially planar and makes angles of 89.4 and 89.1°, respectively, with the equatorial planes of Cu(1) and Cu(2). This ligand exhibits close to two-fold symmetry. The pattern of its C–O bond distances is markedly different: long when O is equatorially coordinated to Cu [1.272(5) and 1.274(5) Å for C(31)–O(1) and C(35)–O(5), respectively], short when O forms a long axial bond to Cu [1.233(5) and 1.239(5) Å for C(32)–O(2) and C(34)–O(4), respectively] and the shortest value for uncoordinated O [1.209(5) Å for C(33)–O(3)]. These structural features were also observed in the bis-chelating croconato group of the copper(II) dimer $[Cu_2(bpca)_2(H_2O)_2(C_5O_5)]\cdot 3H_2O$ (**3**).[15]

The intramolecular Cu(1) ··· Cu(2) separation across the croconato bridge is 6.852(1) Å [6.824(1) Å in **3**], a value which is somewhat shorter than the shortest intermolecular copper–copper distance [7.019(1) Å for Cu(1) ··· Cu(2a); (a) $x - 1$, *y*, *z*].

$[Cu_3(phen)_5(C_5O_5)_2](CF_3SO_3)_2$ (2). The structure of complex **2** is built of croconato-bridged trinuclear $[Cu_3(phen)_5(C_5O_5)_2]^{2+}$ complex ions (Fig. 3 and Table 3) and triflate counter ions which are held together by electrostatic forces. Chains of neighbouring trinuclear units related by centres of symmetry are arranged such that pairs of phenanthroline groups N(1)–C(12) overlap to a considerable extent, the average interplanar spacing between phen groups in positions *x*, *y*, *z* and $0.5 - x$, $0.5 - y$, $1 - z$ being 3.33 Å, indicating a significant π–π interaction (Fig. 4). This arrangement is also stabilized by an O ··· H–C interaction between croconate and the stacked phen group [2.33 Å for O(5) ··· H(8b); (b) $0.5 - x$, $0.5 - y$, $1 - z$]. A two-fold rotation axis runs through the central copper atom and its coordinated phen ligand.

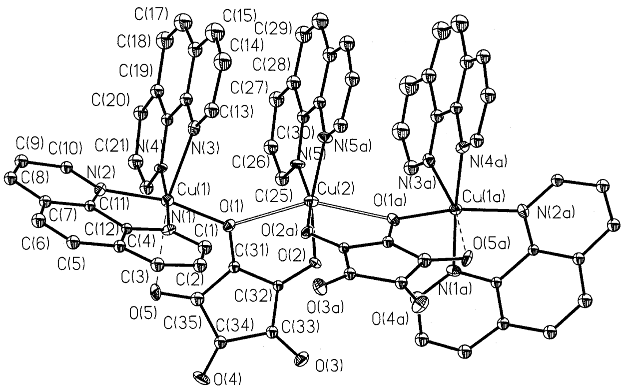

Fig. 3 The trinuclear complex unit $[Cu_3(phen)_5(C_5O_5)_2]^{2+}$ in **2**. Thermal ellipsoids are plotted at the 30% probability level. Hydrogen atoms have been omitted for clarity.

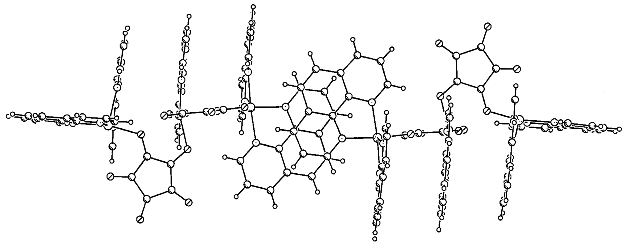

Fig. 4 Arrangement of neighbouring molecules in **2**, depicting the possible π–π interactions between phen groups. The pattern is repeated within chains of molecules.

The terminal copper atom [Cu(1)] has, to the first approximation, a square pyramidal coordination geometry with one croconato oxygen [O(1)] and three phen nitrogen atoms [N(1), N(2) and N(4)] in equatorial positions [Cu(1)–O(1) = 1.970(5), Cu–N in the range 2.009(7)–2.016(7) Å], and a fourth phen nitrogen [N(3)] in the apical position [Cu(1)–N(3) = 2.241(7) Å]. A second, semi-coordinated croconate oxygen atom [O(5)] is situated in the remaining axial position [Cu(1)–O(5) = 2.875(6) Å]. The central copper atom [Cu(2)] has elongated octahedral geometry with two croconate oxygen atoms [O(2) and O(2a)] and two phen nitrogen atoms [N(5) and N(5a)] in equatorial positions [Cu(2)–O(2) = 1.974(6), Cu(2)–N(5) = 2.002(7) Å], and oxygen atoms from the two croconate groups [O(1) and O(1a)] in axial positions [Cu–O(1) = 2.484(5) Å]. The equatorial plane of the terminal copper, Cu(1), has a slight tetrahedral distortion (atomic deviations from mean plane being 0.105–0.115 Å) with the copper atom displaced 0.086 Å from the plane towards the apical nitrogen atom. The central copper, Cu(2), displays a much more pronounced tetrahedral distortion (atomic deviations 0.254–0.276 Å). The dihedral angle between the equatorial planes of the two metal atoms is 74.6°.

The phen groups are all approximately planar and the bond lengths and angles within them are as expected. They act as bidentate ligands, the values of the angles subtended the copper atoms being 82.0(3) and 79.4(3)° [at Cu(1)] and 82.4(4)° [at Cu(2)]. The triflate ions are in the staggered conformation and their bond distances are also as expected [C–F 1.310(11)–1.340(11), S–O 1.413(7)–1.466(7) and S–C 1.810(11) Å]. The croconate ligand is planar and it makes dihedral angles of 88.6 and 88.9° with the two copper equatorial planes. It acts as a bridging ligand through three [O(1), O(2) and O(5)] of its five oxygen atoms. O(1) of the croconate forms a mono-atomic bridge between the two copper atoms, binding in an equatorial position to Cu(1) and in an axial position to Cu(2) [the Cu(1)–O(1)–Cu(2) angle being 139.1(3)°]. At the same time, however, the croconate bridges in the μ-1,2 mode, providing a Cu(1)–O(1)–C(31)–C(32)–O(2)–Cu(2) pathway between the two copper atoms in which both oxygen atoms bind in equatorial positions. Finally, O(5) is weakly coordinated to Cu(1). This bridging mode of croconate was recently observed in two copper(II) compounds, the tetranuclear complex $[Cu_2(L^1)(C_5O_5)]_2$[26] and the sheetlike polymer $[Cu_4(L^2)(C_5O_5)_2]\cdot 6H_2O$[27] ($L^1$ and L^2 are bis-terdentate oxamidate ligands). However, in these two cases, the monoatomic bridge O(1) fills an axial position of each copper atom and the O(2) and O(5) atoms occupy equatorial positions. The carbonyl bonds of the free O(3) and O(4) atoms, and that of the weakly coordinated O(5) atom, are significantly shorter [1.219(10), 1.222(10) and 1.235(10) Å for C(33)–O(3), C(34)–O(4) and C(35)–O(5), respectively] than those of the oxygen atoms coordinated to copper in equatorial positions [1.296(9) and 1.270(9) Å for C(31)–O(1) and C(32)–O(2), respectively]. The lengthening of the C(33)–C(34) [1.518(12) Å] and C(34)–C(35) [1.511(12) Å] intra-ring croconate bonds as compared to the remaining carbon–carbon bond distances [values varying in the range 1.434(11)–1.449(12) Å] is in agreement with a greater bond order for the free carbonyl bonds.

The intramolecular Cu(1) ··· Cu(2) separation across the croconate bridge is 4.177(1) Å, a value much shorter than that observed in **1** because of the different bridging modes of croconate in **1** and **2**. The two terminal copper atoms in **2** are separated by 8.350(1) Å, the angle Cu(1)–Cu(2)–Cu(1a) being 177.0(1)°. The shortest intermolecular copper–copper distance is 8.148(2) Å [Cu(1) ··· Cu(1b)].

Infrared spectra

In addition to the bands attributable to the presence of terpy (1470m, 1450m, 1415m, 770m) and uncoordinated nitrate anions (1380s) (**1**), and phen (3070w, 2910w, 1425m, 1220m, 850m, 725m) and uncoordinated triflate anions (1270s,br, 1030m, 770w, 635m, 520w) (**2**), the infrared spectra of complexes **1** and **2** exhibit a very strong and broad absorption centered at 1550 cm^{-1} which is due to a combination of C–O and C–C bond stretching vibrations of croconate. This type of absorption occuring in the range 1600–1500 cm^{-1} is characteristic of the salts of $C_nO_n^{2-}$ ion (n = 4–6).[45] Additional weak bands are observed above 1700 cm^{-1} [1720 cm^{-1} in **1** and 1735, 1725 and 1710 cm^{-1} in **2**] which are taken as evidence for the presence of uncoordinated carbonyl groups of the croconate entity.[5,9,15,19] The occurrence of coordinated carbonyl groups[9,15,19,22] is characterized by medium strength absorptions at 1665 cm^{-1} in the spectrum of **1**, and at 1660 cm^{-1} with a shoulder at 1650 cm^{-1} for **2**. These spectroscopic features support different coordination modes for croconate in **1** and **2**, as confirmed by the X-ray structural characterisation.

Magnetic properties

The magnetic properties of complexes **1** and **2** in the form of $\chi_M T$ [χ_M being the magnetic susceptibility per two (**1**) and three (**2**) copper(II) ions] are shown in Fig. 5 and 6, respectively. At room temperature, $\chi_M T$ for **1** is 0.84 cm^3 K mol^{-1}, a value which is as expected for two magnetically isolated spin doublets. The value of $\chi_M T$ for **1** remains practically constant when cooling and decreases sharply at $T < 25$ K, reaching a value of 0.30 cm^3 K mol^{-1} at 1.9 K. A maximum in the susceptibility is observed at 2.6 K in the χ_M *versus* T curve (see insert of Fig. 5). These magnetic features of complex **1** are typical of a weak intramolecular antiferromagnetic coupling between two spin doublets. $\chi_M T$ for **2** at 300 K is 1.07 cm^3 K mol^{-1}, a value somewhat below that expected for three non-interacting spin doublets. Upon cooling, the value of $\chi_M T$ continuously decreases, reaches a plateau in the temperature range $5 \le T \le 12$ K with $\chi_M T$ = 0.42 cm^3 K mol^{-1} and slightly decreases at lower temperatures (see insert of Fig. 6). This curve is typical of an intermediate intramolecular antiferromagnetic coupling in a copper(II) trimer, the low-lying spin doublet (plateau of $\chi_M T$) being fully populated at $T \le 12$ K. The slight decrease in $\chi_M T$ at $T < 5$ K is due to the occurrence of very weak intermolecular magnetic interactions.

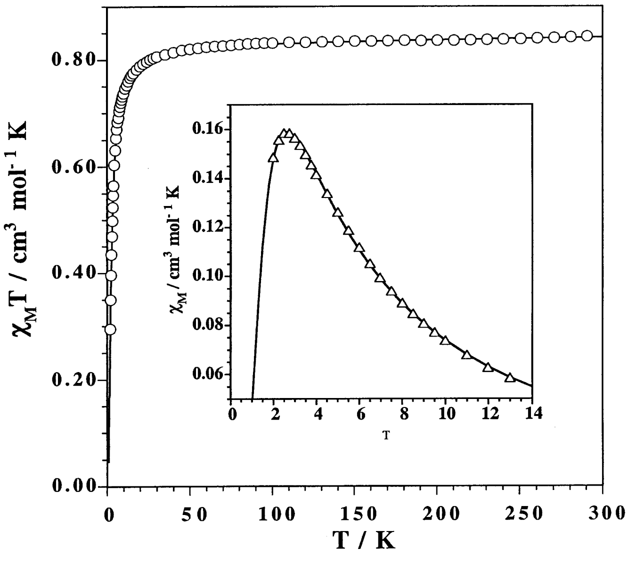

Fig. 5 Thermal dependence of $\chi_M T$ (o) for complex **1**; the solid line is the best fit (see text). The insert shows the susceptibility curve (Δ) in the low temperature region.

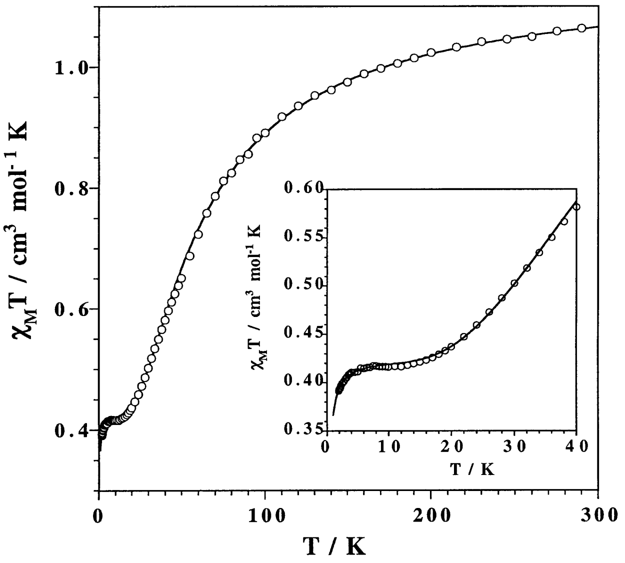

Fig. 6 Thermal dependence of $\chi_M T$ for complex **2**: (o) experimental data; (——) best fit (see text). The insert shows the $\chi_M T$ curve in the low temperature range.

In the light of these considerations, the magnetic data for **1** were analysed through a simple Bleaney–Bowers expression for a copper(II) dimer [eqn (1)] which is derived from the isotropic Hamiltonian in eqn. (2)

$$\chi_M = (2N\beta^2 g^2/kT)[3 + \exp(-J/kT)]^{-1} \tag{1}$$

$$H = -JS_1 \cdot S_2 \tag{2}$$

where N, g and β have their usual meanings, and J is the exchange coupling parameter. Best-fit parameters are: J = −2.9 cm^{-1}, g = 2.11 and $R = 1.7 \times 10^{-5}$ {R is the agreement factor defined as $\Sigma_i[(\chi_M)_{obs(i)} - (\chi_M)_{calc(i)}]^2/\Sigma_i[(\chi_M)_{obs(i)}]^2$}. The calculated curve reproduces the magnetic data very well. The magnetic data for complex **2** were analysed through the expression for a copper(II) trimer [eqn. (3)–(7)][46]

$$\chi_M = \frac{N\beta^2}{4k(T-\theta)} \frac{[g^2_{|1/2,1>} + g^2_{|1/2,0>}\exp(2x) + 10\, g^2_{|3/2,1>}\exp(3x)]}{[1+\exp(2x)+2\ \exp(3x)]} \tag{3}$$

with

$$g_{|1/2,1>} = (4g_2 - g_1)/3 \tag{4}$$

$$g_{|1/2,0>} = g_1 \tag{5}$$

$$g_{|3/2,1>} = (g_1 + 2g_2)/3 \tag{6}$$

and

$$x = J/2kT \tag{7}$$

which was derived from the isotropic Hamiltonian in eqn. (8)

$$H = -J_{12}S_1 \cdot S_2 - J_{13}S_1 \cdot S_3 \tag{8}$$

$J = J_{12} = J_{13}$ is the exchange coupling parameter between adjacent copper(II) ions within the trimer, θ is the parameter accounting for the intermolecular interactions and g_1 (central) and $g_2 = g_3$ (peripheral) are the local Landé factors. The magnetic coupling between the peripheral copper(II) ions (J_{23}), which are separated by 8.350(1) Å [Cu(1) ··· Cu(1a)], was not considered in eqn (8). Best-fit parameters through eqn (3) are: $J = -47.1$ cm^{-1}, $g_1 = 2.06$, $g_2 = 2.11$, $\theta = -0.16$ K and $R = 4.1 \times 10^{-5}$ (R is the agreement factor defined as $\Sigma_i[(\chi_M T)_{obs(i)} - (\chi_M T)_{calc(i)}]^2/\Sigma_i[(\chi_M T)_{obs(i)}]^2$). The calculated curve (solid line in Fig. 6) matches the magnetic data very well.

We conclude this contribution with some comments concerning firstly, the ability of croconato to mediate magnetic interactions between magnetic centers when acting as a bis-chelating bridge and secondly, the different magnitude of the antiferromagnetic coupling through bridging croconato in **1** and **2**. The weak antiferromagnetic coupling observed in **1** can be rationalized on the basis of a simple magnetic orbital picture. The unpaired electron on each copper atom in **1** is mainly delocalized in the equatorial plane and it is described by a $d_{x^2-y^2}$ magnetic orbital [the x and y-axes being roughly defined by the Cu–N bonds]. The admixture of the d_{z^2} orbital in the $d_{x^2-y^2}$ ground state is assumed to be weak because of the long axial distances around each copper atom. The overlap integral (S) between the magnetic orbitals centered on each copper atom through the O(1)C(31)C(35)O(5) σ-type exchange pathway (copper–copper separation larger than 6.8 Å) is expected to be very weak. Consequently, in the approximation where $J \propto S^2$,[47] the magnetic interaction would be very small, as observed. Previous molecular orbital calculations on the parent compound $[Cu_2(bpca)_2(H_2O)_2(C_5O_5)]\cdot 3H_2O$ (**3**),[15] with the same coordination mode for the croconato, have substantiated these points. In spite of the structural similarity between **1** and **3**, a somewhat larger antiferromagnetic coupling ($J = -9.6$ cm^{-1}) is observed in this latter compound, which cannot be explained only in terms of its slightly shorter copper–copper separation across croconato [6.852(1) Å in **1** *versus* 6.824(1) Å in **3**]. Most likely, subtle factors such as the different electronegativity of the amidate nitrogen of bpca and the inner pyridyl nitrogen of terpy modify the spin density on the atoms of the bridge and, thus, change the value of the magnetic coupling. Examples of the fine influence exerted by the electronegativity of the peripheral donors on the value of the magnetic coupling between first-row transition metal ions across oxalato and oxalato-type bridges are known.[48]

The antiferromagnetic coupling in **2** ($J = -47.1$ cm^{-1}) is the strongest reported to date dealing with croconato-bridged complexes. An inspection of the structure of **2** shows that two exchange pathways are operative: one involves the monoatomic O(1) atom (μ-1,1) and the other the O(1)C(31)C(32)O(2) skeleton (μ-1,2). Given that O(1) is equatorially bound to Cu(1), but axially to Cu(2), and that O(2) is equatorially bound to Cu(2), the latter pathway seems to be better adapted to mediate magnetic interactions between the spins of Cu(1) and Cu(2). However, the significant tetrahedral distortion of the environment of Cu(2) would cause a non-negligible admixture of d_{z^2} orbital [the z-axis being defined by the Cu(2)–O(2) axial bond] in the $d_{x^2-y^2}$ ground state of this atom. This feature and the large angle at the O(1) bridge [139.1(3)°] allows us to assume that it could be as efficient as the more extended pathway. This assumption is confirmed by the magneto-structural study of the copper(II) dimer of formula $[Cu_2(phen)_4(C_4O_4)](CF_3SO_3)_2\cdot 3H_2O$ (**4**),[49] which can be taken as a good model for the polyatomic bridging pathway in **2**. In compound **4**, the squarato adopts the μ-1,2-bridging mode, the bridging squarate oxygen atoms being equatorially bound to each copper atom, as are O(1) and O(2) in **2**. The magnetic coupling in **4** is $J = -26.4$ cm^{-1} and, consequently, the difference between this value and that observed in **2** ($J = -47.1$ cm^{-1}) would measure the contribution of the monoatomic bridging pathway. With the lack of magneto-structurally characterised examples of these asymmetric μ-1,1-croconato-bridged systems, the present study demonstrates that it could mediate significant magnetic interactions.

Acknowledgements

This work was supported by the Research Council of Norway and the University of Bergen (purchase of X-ray equipment) and the Spanish Ministry of Science and Technology through project BQU2001–2928.

References

1 L. Gmelin, *Ann. Phys. (Leipzig)*, 1825, **4**, 31.
2 J. D. Dunitz, P. Seiler and W. Czechtizky, *Angew. Chem., Int. Ed.*, 2001, **40**, 1779.
3 N. S. Gonçalves, P. S. Santos and I. Vencato, *Acta Crystallogr., Sect. C*, 1996, **52**, 622.
4 N. C. Baenziger and J. J. Hegenbarth, *J. Am. Chem. Soc.*, 1964, **86**, 3250.
5 R. West and H. Y. Niu, *J. Am. Chem. Soc.*, 1963, **85**, 2586.
6 M. D. Glick, G. L. Downs and L. F. Dahl, *Inorg. Chem.*, 1964, **3**, 1712.
7 M. D. Glick and L. F. Dahl, *Inorg. Chem.*, 1966, **5**, 289.
8 P. R. Schleyer, K. Najafian, B. Kiran and H. Jiao, *J. Org. Chem.*, 2000, **65**, 426.
9 I. Castro, J. Sletten, J. Faus and M. Julve, *J. Chem. Soc., Dalton Trans.*, 1992, 2271.
10 I. Castro, J. Faus, M. Julve, M. Mollar, A. Monge and E. Gutiérrez-Puebla, *Inorg. Chim. Acta*, 1989, **161**, 97.
11 I. Castro, J. Faus, M. Julve, M. Carmen Muñoz, W. Díaz and X. Solans, *Inorg. Chim. Acta*, 1991, **179**, 59.
12 I. Castro, J. Faus, M. Julve and A. Gleizes, *J. Chem. Soc., Dalton Trans.*, 1991, 1937.
13 I. Castro, J. Faus, M. Julve, Y. Journaux and J. Sletten, *J. Chem. Soc., Dalton Trans.*, 1991, 2533.
14 X. Solans, M. Aguiló, A. Gleizes, J. Faus, M. Julve and M. Verdaguer, *Inorg. Chem.*, 1990, **29**, 775.
15 I. Castro, J. Sletten, J. Faus, M. Julve, Y. Journaux, F. Lloret and S. Alvarez, *Inorg. Chem.*, 1992, **31**, 1889.
16 M. Aguiló, X. Solans, I. Castro, J. Faus and M. Julve, *Acta Crystallogr., Sect. C*, 1992, **48**, 802.
17 M. L Calatayud, I Castro, J. Sletten, F. Lloret and M. Julve, *Inorg. Chim. Acta*, 2000, **300–302**, 846.
18 P. Castan, D. Deguenon and F. Dahan, *Acta Crystallogr., Sect. C*, 1991, **47**, 2656.
19 I. Castro, J. Sletten, L. K. Glærum, F. Lloret, J. Faus and M. Julve, *J. Chem. Soc., Dalton Trans.*, 1994, 2777.
20 J. Sletten and O. Bjørsvik, *Acta Chem. Scand.*, 1998, **32**, 770.
21 D. Deguenon, P. Castan and F. Dahan, *Acta Crystallogr., Sect. C*, 1991, **47**, 433.
22 D. Deguenon, G. Bernardelli, J. P. Tuchagues and P. Castan, *Inorg. Chem.*, 1990, **29**, 3031.
23 Q. Chen, S. Liu and J. Zubieta, *Inorg. Chim. Acta*, 1990, **175**, 241.
24 A. Cornia, A. C. Fabretti, A. Giusti, F. Ferraro and D. Gatteschi, *Inorg. Chim. Acta*, 1993, **212**, 87.
25 G. Speier, E. Speier, B. Noll and C. G. Pierpont, *Inorg. Chem.*, 1997, **36**, 1520.
26 G. L. Abbati, A. Cornia and A. C. Fabretti, *Acta Crystallogr., Sect. C*, 1999, **55**, 2043.
27 I. Castro, M. L. Calatayud, J. Sletten, M. Julve and F. Lloret, *C. R. Acad. Sci. Paris, Chim.*, 2001, **4**, 235.
28 J. C. Trombe and C. B. Cabarrecq, *C. R. Acad. Sci., Ser. II*, 1990, **310**, 521.
29 C. B. Cabarrecq and J. C. Trombe, *C. R. Acad. Sci., Ser. II*, 1990, **311**, 1179.
30 C. B. Cabarrecq and J. C. Trombe, *Inorg. Chim. Acta*, 1992, **191**, 227.
31 C. B. Cabarrecq and J. C. Trombe, *Inorg. Chim. Acta*, 1992, **191**, 241.
32 L. M. Schwartz, R. I. Gelband and J. O. Yardley, *J. Phys. Chem.*, 1975, **79**, 2246.
33 J. Sletten and M. Julve, *Acta Chem. Scand.*, 1999, **53**, 631.
34 A. Earnshaw, *Introduction to Magnetochemistry*, Academic Press, London, 1968.
35 J. Cosier and F. H. Glazer, *J. Appl. Crystallogr.*, 1986, **19**, 105.
36 (*a*) A. C. T. North, D. C. Phillips and F. S. Mathews, *Acta*

Crystallogr., Sect. A, 1968, **24**, 351; (*b*) G. Kopfman and R. Huber, *Acta Crystallogr., Sect. A*, 1968, **24**, 348.

37 SADABS, v. 2.01, Bruker/Siemens Area Detector Absorption and Other Corrections Program, Siemens Analyical X-ray Instruments Inc., Madison, WI, USA, 1997.

38 (*a*) CAD4-Express, Delft X-ray Diffraction Instruments, Delft, The Netherlands, 1992; (*b*) K. Harms, XCAD, Philipps-Universität Marburg, Germany, 1996.

39 SMART, v. 4.0, and SAINT, v. 4.0, Data Collection and Data Integration Software, Bruker AXS Inc., Madison, WI, USA, 1997.

40 (*a*) G. M. Sheldrick, *Acta Crystallogr., Sect. A*, 1990, **46**, 467; (*b*) G. M. Sheldrick, SHELXTL/PC, v. 5.10, Bruker AXS Inc., Madison, WI, USA, 1998.

41 D. P. Anderson, A. B. Packard and M. Nicholas, *Inorg. Chem.*, 1976, **15**, 1613.

42 M. I. Arriortúa, T. Rojo, J. M. Amigó, G. Germain and J. P. Declercq, *Acta Crystallogr., Sect. B*, 1982, **38**, 1323.

43 T. Rojo, M Vlasse and D. Beltrán-Porter, *Acta Crystallogr., Sect. C*, 1983, **39**, 194; W. Henke, S. Kremer and D. Reinen, *Inorg. Chem.*, 1983, **22**, 2858.

44 J. V. Folgado, E. Coronado, D. Beltrán-Porter, T. Rojo and A. Fuertes, *J. Chem. Soc., Dalton Trans.*, 1989, 237.

45 M. Ito and R. West, *J. Am. Chem. Soc.*, 1963, **85**, 2580.

46 O. Kahn, *Molecular Magnetism*, VCH, Weinheim, Germany, 1993, p. 214.

47 O. Kahn and M. F. Charlot, *Nouv. J. Chim.*, 1980, **4**, 567.

48 P. Román, C. Guzmán-Miralles, A. Luque, J. I. Beitia, J. Cano, F. Lloret, M. Julve and S. Alvarez, *Inorg. Chem.*, 1996, **35**, 3741.

49 I. Castro, M. L. Calatayud, J. Sletten, F. Lloret and M. Julve, *Inorg. Chim. Acta*, 1999, **287**, 173.